Effect of High-density Current Electropulsing on Corrosion-cracking of Titanium Aluminide Intermetallic

Anatolii Babutskyi[1,2], Andreas Chrysanthou[1], Ganna Chyzhyk[2], Maider Garcia de Cortazar[3], Pedro Egizabal[3], Marija Smelina[1]

[1] School of Physics, Engineering and Computer Science, University of Hertfordshire, Hatfield, UK

[2] G.S. Pisarenko Institute of Problems of Strength, National Academy of Sciences of Ukraine, Kyiv, Ukraine

[3] TECNALIA, San Sebastián, Spain

Correspondence: Ganna Chyzhyk, G.S. Pisarenko Institute of Problems of Strength, National Academy of Sciences of Ukraine, 2 Timiryazevs'ka Str, 01014 Kyiv, Ukraine

Email: anna_chyzhyk@ukr.net

Abstract

The effect of electropulsing on the corrosion-cracking of titanium aluminide produced by self-propagating high-temperature synthesis has been investigated. The electropulsing treatment led to improved corrosion resistance in sodium fluoride solution and also eliminated corrosion cracking at the α_2/γ interface during corrosion in a solution of nitric and hydrofluoric acids. This behaviour was attributed to thermal and athermal effects resulting from electropulsing and leading to the interaction of conduction electrons with the defect structure. Effect of magnetic field accompanying electropusling on depinning of dislocations also has been discussed. Support for this is provided based on X-ray diffraction analysis and microhardness testing.

Keywords: titanium aluminide intermetallic, corrosion, corrosion cracking, residual stress, electropulsing

1 INTRODUCTION

Ti-6Al-4V alloy is commonly used as an implant material in dentistry owing to its good biocompatibility. However, its use has led to some concerns due to its relatively low wear resistance [1,2] and to the possible release of toxic vanadium ions into the body. [3] Alternative vanadium-free titanium alloys based on γ-TiAl intermetallic are therefore being considered for implant applications. γ-TiAl intermetallics were originally developed for aerospace and automotive applications in order to utilize their low density of around 3.8 $Mg \cdot m^{-3}$, high specific strength, high creep resistance and high-temperature capability. [4,5] Their poor fracture toughness and low workability were the main reasons that prevented the development of these materials. One of the most interesting of the γ-TiAl intermetallics is based on the chemical composition Ti–48Al–2Nb–2Cr (at. %) which has improved plasticity, while recent research has demonstrated its biocompatibility in vitro [6] and in vivo. [7] One of the main requirements of dental implant materials is corrosion resistance particularly when exposed to fluoride compounds found in mouth rinses and toothpastes as well as in drinking water and tea. [8] The presence of crystalline defects and dislocations are factors that can have a detrimental effect on the corrosion resistance in metallic materials. Conventionally, thermal post-treatment is used for stress-relief and removal of dislocations. However, thermal treatment can be expensive and can also lead to effects that may be difficult to control like the growth of an oxide layer. During recent years, alternative low-temperature techniques like electropulsing treatment have been under investigation. For example, Zhu et al. [9] and Qin et al. [10] have demonstrated that the use of room-temperature high-energy electropulsing can reduce stresses, alter microstructures and accelerate phase transformations in metals. The use of a pulsed electric current rather than

a direct current (DC) is preferred because a short pulsed current will minimize the Joule heating effect and therefore prevent the development of high temperatures. [11,12] While investigations on the application of the technique have focused on conventional materials, little work has been reported on advanced materials like intermetallics and corrosion. The work which is presented in this paper concerns the effect of electropulsing on the corrosion-cracking in a γ-TiAl-based alloy that had been produced by self-propagating synthesis (SHS).

2 EXPERIMENTAL

Ti–48Al–2Nb–2Cr (at. %) intermetallic was prepared by SHS using mixed elemental powders which had been pressed together into a billet measuring 40 mm x 30 mm x 13 mm. Details of the particle size and purity of the elemental powders are shown in Table 1.

For the SHS reaction, the samples were placed on a ceramic support and enclosed in a transparent silica chamber in a flowing high-purity argon environment. The reaction was initiated by inductively heating the top side (30 mm x 13 mm) of the billet. By preferentially heating one side of the sample, the wave-propagation mode of SHS was promoted. Upon ignition of the reaction, glowing of the samples was observed; at that point the power was switched off and the self-sustaining reaction was allowed to proceed on its own accord. The reaction proceeded by the wave mechanism of SHS and was complete within about 5 seconds. Following cooling, representative samples measuring 25 mm x 6 mm x 3 mm were sectioned from the SHS products by means of electrical discharge machining and polished to a 3 μm polish.

Electropulsing was applied to two samples by passing one pulse of an electric current along the length of the samples using the set up illustrated in Figure 1. A Rogowski belt was used to register the pulsed electric current which was in the form of a decaying sinusoid of total duration of about 400 μs with a peak current of approximately 82 kA. Chromel-alumel thermocouples

(K-type) made of 0.2 mm wires were used to register the temperature at the centre of the larger face of the specimens. As a result of electropulsing, a maximum temperature of 421 °C was recorded for the first sample and 426 °C for the second one.

X-ray diffraction (XRD) analysis was conducted for samples in the initial and electropulsed states using a DRON 3M diffractometer with Cu-Kα radiation of wavelength of 0.154056 nm. Scans were performed for 2θ angles from 20° to 140° at one-second intervals. The samples that were destined for corrosion testing were further polished to a 0.25 μm finish.

Corrosion immersion tests were carried out in polypropylene flasks in a solution of 0.9 % NaF as this concentration is representative of the amount of fluoride used in commercial toothpastes and mouthwashes. The amount of the 0.9 % NaF solution used was 1 mm^3 per 16 mm^2 of the specimen surface area. All the flasks were placed into a circulating water bath at a controlled temperature of 37 ^oC (±1 ^oC) for 120 hours.

The concentrations of the released metal ions (Ti and Al) in solution after the corrosion immersion tests were measured by Inductive-Coupled Plasma Optical Emission Spectrometry (ICP) supplied by Varian 710-ES, Japan. The corrosion behaviour of samples was further examined by etching representative polished samples using a solution of 14 % nitric and 4 % hydrofluoric acids at room temperature. Microhardness measurements were conducted by using a Leitz GMBH Wetzlar 060-366.0 microhardness tester.

3 RESULTS AND DISCUSSION

XRD patterns of the SHS intermetallic products prior to and after electropulsing are presented in Figures 2a and 2b which, as expected, show the presence of γ-TiAl and α_2-Ti_3Al. From Figure 2b it is evident that following electropulsing, the XRD peaks had shifted slightly to the left and also became less broad.

Corrosion tests were undertaken using two samples each for the untreated and the electropulsed conditions by immersing in a 0.9 % NaF solution. The effect of corrosion based on ICP measurements of the concentration of the released titanium and aluminium ions into solution are shown in Table 2. It is apparent that the material loss was lower for the samples that had undergone electropulsing indicating that the application of the technique had increased the corrosion resistance of the material.

The corrosion behaviour was further examined by etching representative polished samples using a solution of 14 % nitric and 4 % hydrofluoric acids. Examination of the etched surface by means of light microscopy revealed evidence of the development of several microcracks on the etched surface of the untreated samples as shown in Figure 3a. The microcracks occurred at the interface between the alternating γ-TiAl and α_2-Ti_3Al phases. This type of behaviour is similar to stress-corrosion cracking which typically occurs as a result of the presence of dislocations at grain boundaries in metals. The etched samples that had been subjected to electropulsing exhibited a significant reduction in the number of microcracks and in fact showed no evidence of microcracking at the α_2/γ interface at all as presented in Figure 3b. The only microcracks that occurred in the samples that had undergone electropulsing were situated at the interface of the α_2/γ clusters.

The observation that the electropulsed samples had improved corrosion resistance and that upon etching they showed no microcracking at the α_2/γ interface suggested that electropulsing had led to a reduction in the number of dislocations and in the interfacial microstraining. In order to verify this, microhardness tests were carried out and it was observed that following electropulsing, there was a significant drop in the microhardness from HV 357 to HV 284. Inspection of the XRD patterns in Figures 2a,b also revealed that following electropulsing, the XRD peaks had shifted slightly to the left and also became less broad. A decrease in the breadth of the peaks is associated with an increase in the coherent scattering domain size and

with a reduction in the number of defects like dislocations in the structure. These effects can be analyzed using the Williamson-Hall equation which is presented below:

$$\beta \cos \theta = (\lambda / L) + 4\varepsilon \cdot \sin \theta \,, \quad (1)$$

where β is the width of the X-ray half-peaks in radians, θ is the angle of diffraction, λ is the wavelength of the XRD beam, L is the coherent scattering domain size and ε is the microstrain present in the material. A plot of $\beta \cdot \cos \theta$ against $\sin \theta$ shows a linear relationship with a slope equal to 4ε and intercept (λ/L). While this approach may not necessarily yield absolute microstrain values (owing to the various assumptions in its derivation), it can be used to assess the relative nature of a material.

The obtained data for γ-TiAl show that electropulsing led to a decrease from $4.91 \cdot 10^{-2}$ to $2.74 \cdot 10^{-2}$ in the microstrain, while in the case of the α_2-Ti_3Al the change was from $1.96 \cdot 10^{-2}$ to $1.50 \cdot 10^{-2}$. These measurements are indicative of a reduction in the number of dislocations in the α_2/γ aluminide. In addition, an increase in the coherent scattering domain size was observed from 14.67 nm to 19.01 nm for γ-TiAl and from 8.10 nm to 10.51 nm for α_2-Ti_3Al.

The shift of the diffraction peaks to a lower angle indicated that there was an increase in the lattice parameters of the constituent phases as a result of electropulsing. This was accompanied with an increase in the c/a ratio of the face-centred tetragonal γ-TiAl from an initial value of 1.0170 to 1.0180 following electropulsing. The relatively fast cooling of the SHS product is likely to lead to tetragonal distortion in the γ-TiAl lattice and to a less ordered crystal lattice as previously reported by Whang and Li. [13] The observed increase in the c/a ratio indicated that electropulsing resulted in more ordering in the γ-TiAl phase. The application of electropulsing provided sufficient energy for electromigration and some rearrangement of atoms and a reduction in the number of dislocations. Similarly the increase in the coherent scattering domain size of γ-TiAl was due to electromigration involving diffusion of atoms to rearrange themselves to form a more ordered state.

The absence of microcracks at the α_2/γ interface implied that there was a change in the α_2/γ interfacial character. From previous research it is known that there is a mismatch of between 1% and 2% at the interface between the γ and α_2 lamellae. [14,15] The misfit strain between α_2 and γ can be solely taken up by elastic distortion if the lamellae are uniformly strained to bring the atomic spacings into registry and this can be achieved for extremely thin lamellae giving a fully coherent interface. According to Hazzledine, [16] the critical lamellar thickness for a fully coherent interface in α_2/γ intermetallics is between 0.8 nm to 3.9 nm.

However, based on the XRD results of the present investigation, the domain sizes of both γ-TiAl and α_2-Ti_3Al were higher than the critical size and in fact increased even further as a result of electropulsing so the conversion from a semi-coherent to a fully coherent interface is unlikely to have taken place. An alternative way of relieving interfacial mismatch strains may be the formation of atomic steps or ledges which may replace misfit dislocations as reported by earlier research. [17,18]

Earlier researchers have reported that both thermal and athermal effects can result when electropulsing is applied to metals [19] and such changes in microstructure may be promoted by these effects. The thermal effect is associated with Joule heating, and an increase in the temperature of the samples during electropulsing indicates this (the recorded increase in the surface temperature of the samples was near 420° C). The recorded temperatures are about 0.4 times the melting point of the intermetallic and therefore Joule heating may lead to diffusion and migration of dislocations. At the same time, thermal diffusion needs time to progress and in the case of the present time was very short; heating to about 420° C was achieved within 400 μs and then the sample was cooled down naturally. This short time is not sufficient for the observed effects to occur and therefore, the athermal effect of the electropulsing process should be considered. The athermal contribution that involves stress relaxation may be attributed to the electroplastic [20,21] and magnetoplastic [22,23] effects

as the sample is exposed both to an electric current and magnetic field as an integral side-effect of the current passing through the sample. For example, in the case of a round sample, the magnitude of the field within it is a function of the current I passing through the sample and the radius r of the sample:

$$B = \mu_0 Ir/(2\pi R^2), \quad (2)$$

where μ_0 = 1.25663706212·10^{-6} H/m is the vacuum permeability and R is the radius of the sample. Following on from Equation (2), the magnetic field attained by the sample is proportional to r and depends on the current. For a round sample with r = 2.39 mm, which cross-section is equal to 3 mm x 6 mm cross-section used in the present research, the magnetic flux density on the sample surface due to the passing of electric current with 82 kA amplitude can be estimated as 6.85 T.

The electroplastic effect can be promoted by the electron wind force that can lead to dislocation motion. This effect of the electric pulse current on the crystal lattice of a metal can be estimated using the following basic relations that determine the kinetics of the interaction of conduction electrons with the crystal lattice in accordance with existing concepts of electrical conductivity [24, 25]:

$$\begin{aligned} i &= e\ vn_0; \\ \frac{dU}{dx} &= E = \rho i; \quad (3) \\ \rho &= \frac{2m_e}{n_0 e^2 t_0}, \end{aligned}$$

where i is the current density in A/m^2, e is the electron elementary charge, v is the velocity of the electron drift in m/s, n_0 is the number of conductivity electrons per unit volume (1/m^3), U is the electric potential in V, E is the electric field intensity in V/m, ρ is the electrical

resistivity in Ω·m, m_e is the electron rest mass which is equal to $9.10956 \cdot 10^{-31}$ kg and t_0 is the mean free time of electrons between ionic collisions. It follows from these equations that the kinetic energy of the electron drift, K_e, under the action of an electric field in isotropic electron scattering can be expressed in the form:

$$K_e = m_e v^2/2 = eE \cdot (vt_0) = \rho i (evn_0)\frac{t_0}{n_0} = \rho i^2 \frac{t_0}{n_0}. \quad (4)$$

Using the equations above, the parameters for the interaction between electrons and the crystal lattice can be estimated. The increase in the kinetic energy of an electron within its free path for titanium as calculated by Equation (4) at the current density of 4.6 kA/mm^2 that was used in the present study yields $\Delta K_{e(Ti)} \cong 2.03 \cdot 10^{-12}$ eV/atom. This value is very small as the change in the thermal motion energy (ΔK_T) at an increase in temperature just by 1°C equals $\Delta K_T \cong kT \cong 8.61 \cdot 10^{-5}$ eV/atom. Thus, a single interaction between an electron and an atom does not significantly affect the motion of the atom in an ideal crystal lattice. At the same time, it can be assumed that there is a preferable interaction between conduction electrons and atoms near dislocation cores and other defects; such interaction contributes to an increase in the mobility of dislocations. This has been confirmed by extensive studies presented by Baranov et al. [26] where the effect of stress relaxation was experimentally established for a wide range of metals at an electric current density > 1 kA/mm^2 (in the present study the current density of 4.6 kA/mm^2 was used under electropulsing).

Molotskii [23] has suggested that the application of a magnetic field to a paramagnetic alloy (Ti and Al are paramagnetic) triggers dislocation movement. It is assumed that this movement occurs as a result of the release of internal (residual) energy that has accumulated in the material during its manufacture. Considering that the bonding energy of dislocation-to-paramagnetic obstacles like impurities, vacancies, etc. depends on the spin multiplicity of the radical pairs spin states (which are in the form of a singlet with high binding energy or a

triplet with low binding energy) that are formed by the dislocation core and the obstacles, it was suggested that the application of a magnetic field may induce a transition from the singlet to a triplet state. This causes an increase in the number of triplet states leading to the dislocation movement by the unpinning of dislocations from obstacles. Such dislocation movement as achieved by the eectropulsing treatment has and provided relief to the α_2/γ interfacial mismatch strains by the formation of atomic steps or ledges and has eliminated cracking during the corrosion process.

Finally, it can be assumed that the natural concentration of an electric current and a magnetic field near defects, such as pores that exist in the samples following SHS, enhances the above-mentioned electroplastic and magnetoplastic effects.

The observed increase in the resistance to general corrosion also may be associated with a decrease in residual stresses, since the mechanism of electrochemical corrosion includes the formation of short-circuited micro galvanic anode-cathode pairs, which can arise for various reasons (roughness, changes in the metal structure, etc.) and in particular, due to residual stresses [27,28].

4 CONCLUSIONS

The investigation that was undertaken has shown that the use of electropulsing of current density of 4.6 kA/mm^2 can lead to an improvement in the corrosion behaviour of TiAl intermetallic. In addition, the use of the technique eliminated corrosion cracking at the α_2/γ interface. At the same time, reduction in both the microhardness and microstraining of the intermetallic were measured. These effects were attributed to the thermal and athermal effects of electropulsing which can stimulate dislocation movement and provide relief to the α_2/γ interfacial mismatch strains by the formation of atomic steps or ledges.

ACKNOWLEDGEMENTS

This work was supported by the Marie Curie International Incoming Fellowship scheme within the 7th European Community Framework Programme Grant number PIIF-GA-2010-274324.

AUTHOR CONTRIBUTIONS

All the authors contributed equally to prepare, develop and carry out this manuscript.

CONFLICT OF INTEREST

The authors declare no financial or commercial conflict of interest.

ORCID

Ganna Chyzhyk https://orcid.org/0000-0003-0561-7651

REFERENCES

[1] J. Li, M. Sun, X. Ma, G.Tang, *Wear* **2006**, *261*, 1247.

[2] D. E. MacDonald, B. E. Rapuano, N. Deo, M. Stranick, P. Somasundaran, A. L. Boskey, *Biomater.***2004**, *25*, 3135.

[3] M. A. Khan, R. L. Williams, D. F. Williams, *Biomater.* **1999**, *20*, 631.

[4] M. Yamaguchi, H. Inui, K. Ito, *Acta Mater.* **2000**, *48*, 307.

[5] E. A. Loria, *Intermetall*. **2000**, *8*, 1339.

[6] C. Delgado-Alvarado, P. A. Sundaram, *Acta Biomater*. **2006**, *2*, 701.

[7] O. Rivera-Denizard, N. Diffoot-Carlo, V. Navas, P. A. Sundaram, *J. Mater. Sci.: Mater. Med.* 2008, 19, 153.

[8] G. Mabilleau, S. Bourdon, M. L. Joly-Guillou, R. Filmon, M. F. Basle, D. Chappard, *Acta Biomater*. **2006**, *2*, 121.

[9] R. S. Qin, A. Rahnama, W. J. Lu, X. F. Zhang, B. Elliott-Bowman, *Mater. Sci. Techn.* **2014**, *30*, 1040.

[10] Y. Zhu, S. To, W. B. Lee, X. Liu, Y. Jiang, G. Tang, *J. Mater. Res.* **2009**, *24*, 2661.

[11] J. P. Barnak, A. F. Spencer, H. Conrad, *Scripta Metall. Mater*. **1995**, *32*, 879.

[12] R. S. Qin, E. I. Samuel, A. Bhowmik, *J. Mater. Sci.* **2011**, *46*, 2838.

[13] S. H. Whang, Z. X. Li, *Mater. Sci. Eng.* **1988**, *98*, 269.

[14] F. Appel, *Recrystallisation*, InTech, Croatia, **2012**.

[15] K. Maruyama, M. Yamaguchi, G. Suzuki, H. Zhu, H. Y. Kim, M. H. Yoo, *Acta Mater.* **2004**, *52*, 5185.

[16] P. M. Hazzledine, *Intermetall*. **1998**, *6*, 673.

[17] M. G. Hall, H. I. Aaronson, K. R. Kinsma, *Surf. Sci*. **1972**, *31*, 257.

[18] J. M. Howe, R. C. Pond, J. P. Hirth, *Progr. Mater. Sci*. **2009**, *54*, 792.

[19] S. To, Y. H. Zhu, W. B. Lee, G. Y. Tang, X. M. Liu, Y. B. Jiang, *Mater. Trans*. **2009**, *50*, 1105.

[20] H. Conrad, Mater. *Sci. Eng. A* **2000**, *287*, 276.

[21] H. Conrad, *Mater. Sci. Eng. A* **2002**, *322*, 100.

[22] V. I. Alshits, E. V. Darinskaya, M. V. Koldaeva, E. A. Petrzhik, *Elsevier* **2008**, *12*, 334.

[23] M. I. Molotskii, *Mater. Sci. Eng. A*, **2000**, *287*, 248.

[24] R. W. Christy, A. Pytte, *The Structure of Matter; An Introduction to Modern Physics*, W. A. Benjamin Inc., New York, Amsterdam, **1965**.

[25] A. Babutskyi, A. Chrysanthou, M. Smelina, G. Stepanov, M. Ziętara, *Mater. Sci. Techn.* **2017**, *33(12)*, 1461.

[26] Y. V. Baranov, O. V. Troitskii, Y. S. Avraamov, A. D. Shlyapin, *Physical Bases of Electric-pulse and Electroplastic Treatments and New Materials*, MGIU, Moscow **2001**.

[27] J. J. Harwood, *Corros.* **1950**, *6*, 249.

[28] O. Takakuwa, H. Soyama, *Adv. Chem. Eng. Sci.* **2015**, *5*, 62.

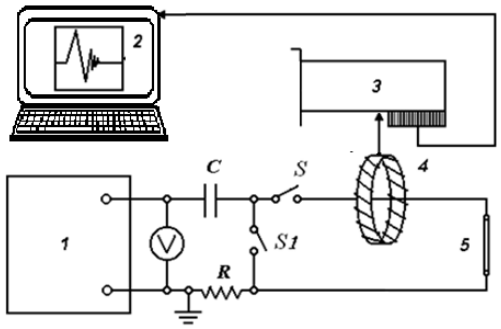

Figure 1. PEC generator scheme: C – capacitor battery, R – ballast resistor, S and S1 – switches; 1 – high voltage supplier, 2 – software, 3 – AD high frequency converter, 4 – Rogowski belt (coil), 5 – specimen

Table 1. Composition and sizes of initial powders used for the production of Ti–48Al–2Nb–2Cr (at. %)

Powder	Size, μm	Chemical composition of the raw materials (wt.%)							
		Ti	Al	Cr	Nb	O	H	C	N
Ti	< 75	99.7	-	-	-	0.229	0.02	0.018	0.016
Al	< 200	-	99.5	-	-	-	-	-	-
Nb	< 45	-	-	-	99.8	0.01	0.0006	0.004	0.003
Cr	< 45	-	0.002	99.89	-	0.067	-	0.005	0.035

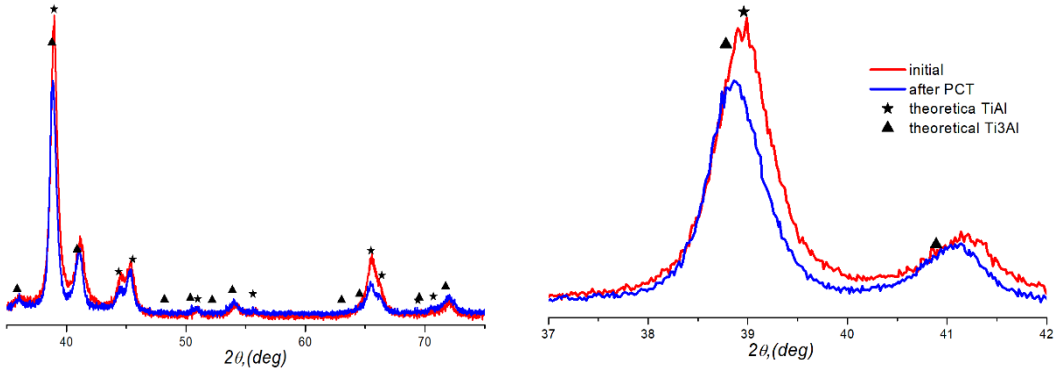

(a) (b)

Figure 2. XRD patterns of the SHS product before and after electropulsing; (a) 2θ from 35° to 75° and (b) 2θ from 37° to 42°

Table 2. Concentrations of Al and Ti ions in solution after 120 hr exposure to 0.9% sodium fluoride solution

Label	Concentration in solution, mg/L				Change of concentration due to electropulsing treatment, %
	Initial state		After electropulsing		
	Mean	Stand. dev.	Mean	Stand. dev.	
Al 237.312	3.24302	0.12322	2.75272	0.04618	-15.1
Ti 334.941	15.69831	0.15639	14.04463	0.20634	-10.5

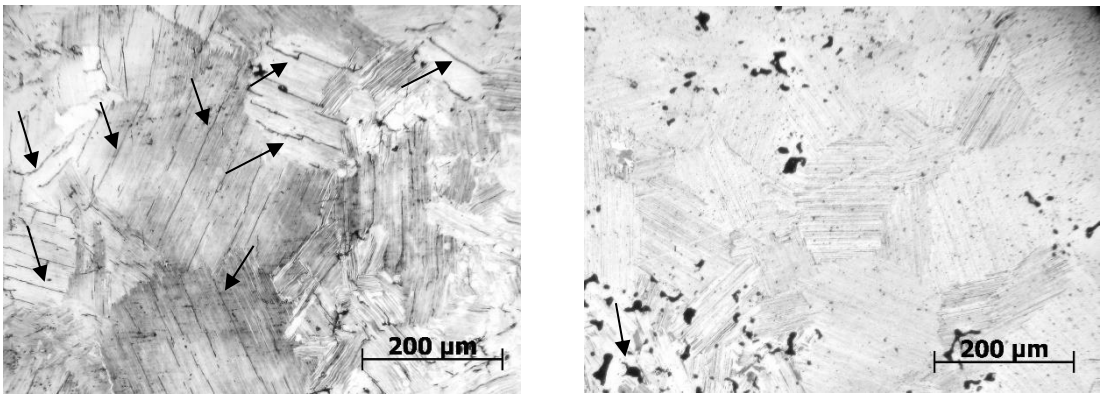

(a) (b)

Figure 3. Microstructure of material following corrosion in 14% HNO3-4%HF solution of samples (a) before electropulsing and (b) after electropulsing. Cracks are marked by arrows.